Photoswitchable Hydrogen-Bonding in Self-Organized Cylindrical Peptide Systems**

Martin S. Vollmer, Thomas D. Clark, Claudia Steinem, and M. Reza Ghadiri*

Molecular self-organization is of paramount importance for the development of functional materials.[1, 2] The desire to control self-assembly processes by external signals, such as light, has led to the design of numerous photochromic supramolecular systems.[3] Among the various photoswitchable molecules, azobenzenes are utilized extensively in supramolecular chemistry, catalysis, and material science because of their efficient, reversible $E \rightarrow Z$ photoisomerization that leads to large changes in molecular geometry.[4–12]

Here we report the synthesis and characterization of the novel peptide system **1** (Scheme 1), in which E/Z isomerization of the azobenzene subunit results in photoswitchable hydrogen bonding, which allows the controlled conversion between inter- and intramolecularly assembled cylindrical structures both in solution and in thin films at the air–water interface.

The peptide system **1** is composed of two cyclic octapeptides with alternating D- and L-α-amino acids bridged by an azobenzene moiety. The peptides were designed to give good solubility in nonpolar organic solvents, to offer a reactive nucleophile (cysteine side chain) for the linkage with the azobenzene, and to limit the self-assembly to dimeric β-sheetlike structures by selective backbone N-methylation.[13] This system was also engineered to exhibit the following structural and kinetic properties. In nonpolar organic solvents, the E isomer of azobenzene ((E)-**1**) was foreseen to exist as an "assembly pool" comprised of dimers and higher oligomers, formed as a result of intermolecular hydrogen bonding and hence concentration dependent (Scheme 1). Irradiation with UV light was expected to cause $E \rightarrow Z$ isomerization and conversion from intermolecular assemblies into the single intramolecularly hydrogen-bonded species (Z)-**1**. Molecular modeling studies indicated that the thioether spacer connecting the peptide and azobenzene moiety would allow optimal formation of eight intramolecular hydrogen bonds. Furthermore, the Z isomer was predicted to confer resistence against thermal $Z \rightarrow E$ isomerization as a consequence of the increased stability offered by intramolecular hydrogen bonding.

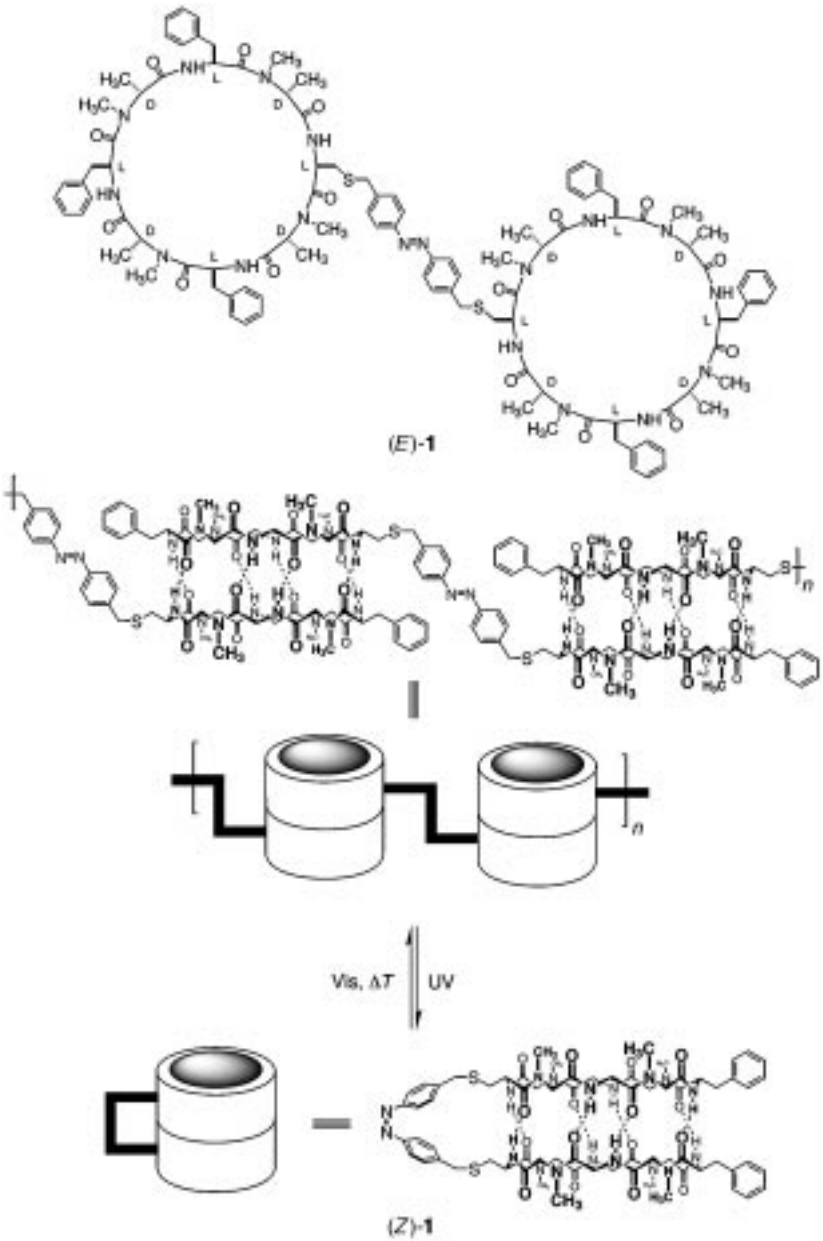

Scheme 1. Peptide sequence employed in this study and schematic representation of the photochemical switching between inter- ((E)-**1**) and intramolecularly ((Z)-**1**) hydrogen-bonded cylindrical aggregates (for clarity most side chains are omitted).

The azobenzene peptide system **1** was synthesized and purified using standard techniques.[14] The characterization was performed by UV/Vis, NMR, and FT-IR spectroscopy, as well as electrospray ionization mass spectrometry (ESI-MS).[15, 21, 23] The photoisomers (E)-**1** and (Z)-**1** show UV/Vis absorption bands characteristic of the azobenzene chromo-

[*] Prof. Dr. M. R. Ghadiri, Dr. M. S. Vollmer, Dr. T. D. Clark, Dr. C. Steinem
Departments of Chemistry and Molecular Biology and
The Skaggs Institute for Chemical Biology
The Scripps Research Institute
10550 North Torrey Pines Road, La Jolla, CA 92037 (USA)
Fax: (+1) 619-784-2798
E-mail: ghadiri@scripps.edu

[**] This work was supported in part by the Office of Naval Research (N00014-94-1-0365) and the National Institute of Health (GM52190). M.S.V. thanks the Deutscher Akademischer Austauschdienst (DAAD) for a NATO Postdoctoral Fellowship and C.S. thanks the Deutsche Forschungsgemeinschaft (DFG) for a Postdoctoral Fellowship. T.D.C. is the recipient of a NSF Predoctoral Fellowship.

  1433-7851/99/3811-1598 $ 17.50+.50/0

phore (Figure 1). The $\pi-\pi^*$ absorption band between 330 and 390 nm of (*E*)-**1**[16] is red shifted by about 6 nm relative to the reference compound (*E*)-4,4′-dimethylazobenzene, which leads to a more selective excitation (96%) of the *E* isomer

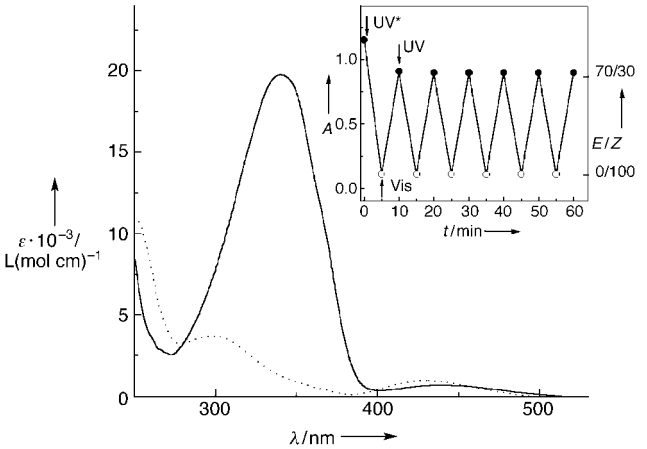

Figure 1. UV/Vis spectra of (*E*)-**1** (—; *E*:*Z* = 90:10, photostationary equilibrium in ambient daylight) and (*Z*)-**1** (⋯; *E*:*Z* = 0:100, photostationary equilibrium at 366 nm) in chloroform at 293 K. The inset shows switching cycles from (*Z*)-**1** (*E*:*Z* = 0:100) to (*E*)-**1** (*E*:*Z* = 70:30) by UV and Vis irradiation (5 min), respectively (the first UV irradiation is marked with an asterix). The absorbance *A* was monitored after each irradiation step.

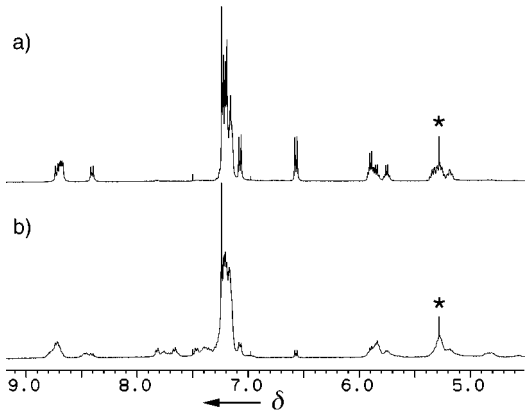

Figure 2. The NH and C$^{\alpha}$H regions of the one-dimensional ^{1}H NMR spectra (400 MHz, 293 K, $CDCl_3$) of a) (*Z*)-**1** (the spectrum was recorded 24 h after switching to the *Z* isomer) and b) a 90:10 mixture of (*E*)-**1** and (*Z*)-**1.** The residual CH_2Cl_2 is marked with an asterisk. a) A single set of sharp resonances are present for (*Z*)-**1**, with downfield shifts for the NH ($\delta = 8.41-8.72$) and C$^{\alpha}$H signals ($\delta = 5.19-5.89$) relative to the related non-assembled cyclic peptides, which indicates the formation of a tight hydrogen-bonded β-sheet structure. The $^3J_{N,\alpha}$ values are all greater than 8.6 Hz, characteristic of β-sheets. b) In the case of (*E*)-**1** several sets of resonances are observed, which is consistent with the presence of multiple oligomeric intermolecular assemblies. The NH and C$^{\alpha}$H signals exhibit downfield shifts similar to (a); however, C$^{\alpha}$H resonances at $\delta > 5$ can be clearly seen, which likely arise from monomeric (*E*)-**1**.

at 366 nm. Remarkably, UV irradiation of (*E*)-**1** at 366 nm[17] causes a quantitative conversion to the *Z* isomer as shown by ^{1}H NMR spectroscopy. Examples of quantitative $E \rightarrow Z$ photo-isomerization are rare.[18] In general, azobenzenes display *E*:*Z* ratios in the range of 50:50[5] to 10:90[3, 19] at the photostationary equilibrium (UV irradiation). On the other hand, irradiation of (*Z*)-**1** with visible light leads to the $Z \rightarrow E$ isomerization with an *E*:*Z* ratio of approximately 85:15 at the photostationary equilibrium.[20]

The 1D and 2D ^{1}H NMR studies establish that (*Z*)-**1** has the expected monomeric hydrogen-bonded cylindrical structure.[13] The 1D NMR spectrum of (*Z*)-**1** is concentration-independent and shows a single set of sharp resonances (Figure 2a).[21] The ROESY spectrum displays only ROE cross peaks (Figure 3a), which indicates a unique structure with no exchange processes detectable on the R_1 time scale.[22] Additionally, the position of the signals corresponding to the *ortho* ($\delta = 6.56$) and *meta* ($\delta = 7.07$) protons confirms the *Z* stereochemistry of the azobenzene.[18] The 1D NMR spectrum of (*E*)-**1** is more complicated than that of (*Z*)-**1**, and denotes, as expected, the presence of several species (Figure 2b).[23] Azobenzene signals now appear in regions diagnostic of a *E* configuration,[18] however, both *ortho* ($\delta = 7.32-7.50$) and *meta* ($\delta = 7.70-7.85$) protons display multiple resonances. In addition, the ROESY spectrum of (*E*)-**1** shows numerous exchange peaks (Figure 3b). These data indicate that (*E*)-**1** predominantly forms intermolecular aggregates such as dimers and/or higher oligomers.

FT-IR studies of (*E*)-**1** and (*Z*)-**1** further support the predominance of hydrogen-bonded β-sheet assemblies in chloroform. The IR data display only one amide A band ($\tilde{\nu}_{N\text{-}H}$) at 3308 cm^{-1} (indicative of hydrogen bonding), the amide $I_{\perp}$ band at 1630 cm^{-1}, and the amide II_{II} band at 1525 cm^{-1}, which are characteristic of β-sheet structures.[13] The expected signals of non-hydrogen-bonded NH stretches in (*E*)-**1** could not be observed by FT-IR spectroscopy. The association behavior of (*E*)-**1** was also studied by ESI-MS. In addition to signals characteristic for the monomer,[14] the appearance of the signals for $[2M+H+Na]^{2+}$ as well as $[2M+H+K]^{2+}$ established the presence of a dimer in the assembly pool.

The photoisomerization of **1** is completely reversible in both directions. This can be demonstrated by irradiation of (*E*)-**1** in chloroform solution first with UV light (366 nm, 5 min) followed by visible light (5 min). The absorption was monitored at 340 nm after each irradiation step (inset of Figure 1). The chosen time intervals for irradiation allow reversible switching between an *E*:*Z* ratio of 0:100 to 70:30 and with longer Vis irradiation[20] beween 0:100 to 85:15.

It was expected that (*Z*)-**1** would be more resistent to thermal $Z \rightarrow E$ isomerization than (*Z*)-4,4-dimethylazobenzene as a result of intramolecular hydrogen bonding. Therefore we investigated the rate constants for the thermal $Z \rightarrow E$ isomerization at different temperatures by UV/Vis spectroscopy and calculated the activation energy E_a from the Arrhenius plot (Table 1). The thermal $Z \rightarrow E$ isomerization of (*Z*)-**1** at 293 K in the dark is 7.5 times slower than that of (*Z*)-4,4′-dimethylazobenzene.

With regard to thin films as components for optical devices, we also investigated the self-organization of the peptide system **1** at the air–water interface. Remarkably, both the *E* and *Z* isomer form very stable thin films. The respective isotherms are readily distinguished by plateau regions at 12.5 mN m^{-1} and 14.0 mN m^{-1}, respectively (Figure 4). Reversible isomerization of **1** within the film is facile as well.

  1433-7851/99/3811-1599 $ 17.50+.50/0

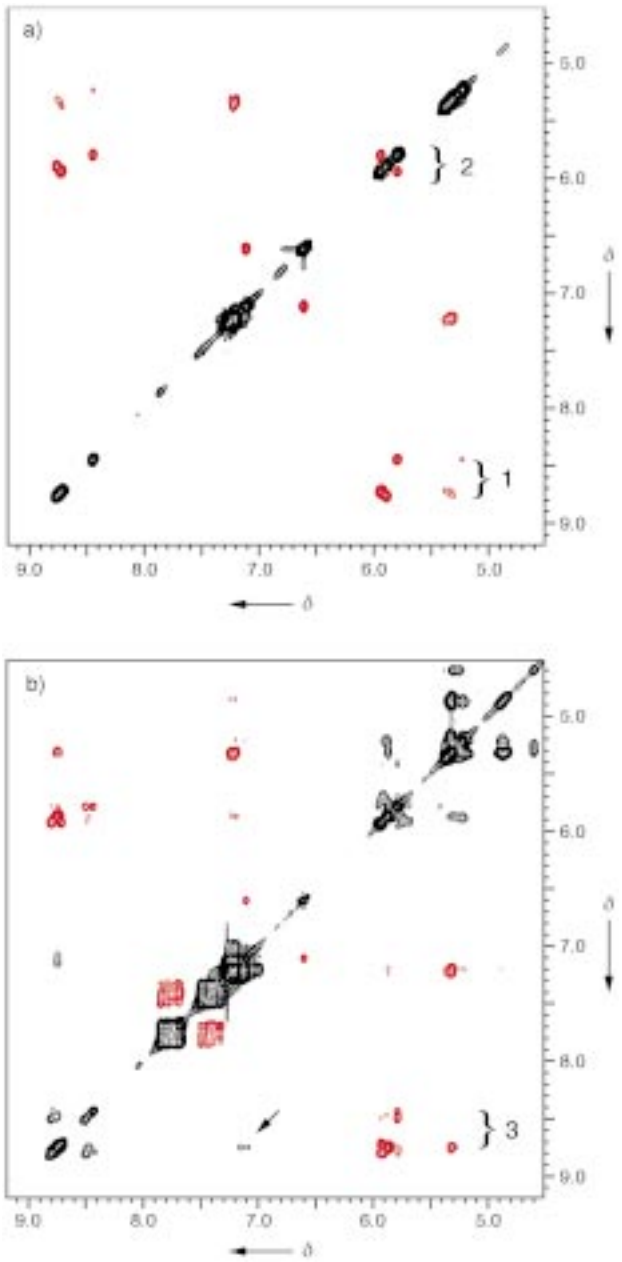

Figure 3. ROESY spectra of (*Z*)-**1** and a 90:10 mixture of (*E*)-**1** and (*Z*)-**1** showing NH, aromatic H, and C$^{\alpha}$H regions. ROE cross peaks are shown in red, while exchange cross peaks are in black. a) (*Z*)-**1** (400 MHz, 293 K, $CDCl_3$). Only ROE cross peaks are observed, which supports the idea of a unique, monomeric species. Area 1 shows strong $d_{\alpha\text{-N}}$ (i, $i+1$) ROE cross peaks (downfield) and weaker intramolecular residue signals (upfield), consistent with the expected β-sheet structure. Furthermore, region 2 displays strong $d_{\alpha\text{-}\alpha}$ cross-strand ROE signals diagnostic of antiparallel β-sheets. b) (*E*)-**1**:(*Z*)-**1** = 90:10 (500 MHz, 293 K, $CDCl_3$). In addition to ROE cross peaks, numerous exchange peaks are observed. For example, area 3 shows a complicated pattern of $d_{\alpha\text{-N}}$ ROE signals and $d_{\text{N-N}}$ exchange peaks, which reflects the presence of multiple interconverting oligomeric species. The exchange cross peaks marked with an arrow occur between hydrogen-bonded and free NH resonances, the latter possibly arising from monomeric (*E*)-**1**.

Switching cycles were carried out while maintaining either a constant area or surface pressure. Under constant area conditions the surface pressure increases by 1.2 mN m^{-1} upon conversion from the *E* into the *Z* isomer (inset of Figure 4).

Table 1. Rate constants k [s^{-1}] of the thermal $Z \rightarrow E$ isomerization of (*Z*)-**1** and (*Z*)-4,4′-dimethylazobenzene (AZO) at different temperatures, as well as the activation energy E_a [kcal mol^{-1}] and the Arrhenius constant $\ln A$ [s^{-1}].[a]

	$k_{293\ K}$	$k_{303\ K}$	$k_{313\ K}$	$k_{323\ K}$	E_a	$\ln A$
(*Z*)-**1**	2.9×10^{-7}	1.1×10^{-6}	3.6×10^{-6}	1.1×10^{-5}	23.4	25.0
AZO	2.2×10^{-6}	7.0×10^{-6}	2.2×10^{-5}	7.1×10^{-5}	22.4	25.3

[a] All experiments were performed in duplicate. The statistical errors are < 5 %.

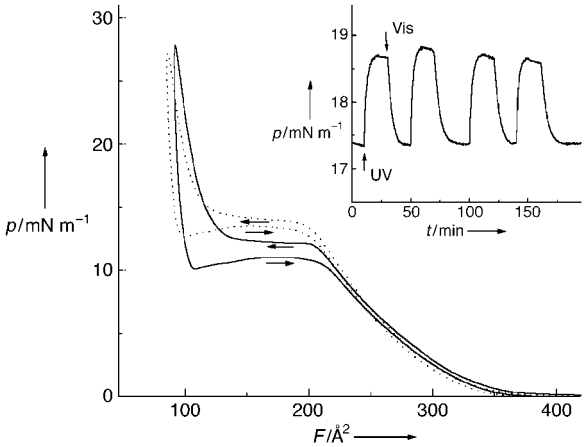

Figure 4. Surface pressure area isotherms (compression and expansion) of (*E*)-**1** (——) and (*Z*)-**1** (····) on water at 293 K; F is the area per molecule. The arrows indicate the direction of compression and expansion. The inset shows four photoinduced isomerization cycles of the peptide film at the air–water interface under constant area conditions. The area per molecule was adjusted to 175 Å^2 after equilibration of the peptide film for 10 h on the air–water interface at 0 mN m^{-1}.

Peptide films were transferred onto a solid support, such as mica and quartz glass, for analysis of the two-dimensional structure by scanning force microscopy and UV/Vis spectroscopy. We observed self-organized photoswitchable peptide films on these surfaces as well.[24]

Altogether, the described azobenzene–peptide **1** provides a new photochromic supramolecular system that permits reversible switching between inter- and intramolecular hydrogen bonds both in solution and in thin films. We anticipate that this structure-based switching principle together with the quantitative conversion into the *Z* isomer will have a number of potential applications including photoswitchable transmembrane channels and ionophores. Furthermore, self-organization of photoswitchable peptides on solid substrates can provide a potential entry to novel photoactive materials as components for optical, electronic, and sensor devices.

Received: November 6, 1998 [Z12630IE]
German version: *Angew. Chem.* **1999**, *111*, 1703–1706

Keywords: azo compounds · hydrogen bonds · peptides · photochromism · supramolecular chemistry

[1] J.-M. Lehn, *Supramolecular Chemistry*, VCH, Weinheim, **1995**.
[2] a) J. S. Lindsey, *New. J. Chem.* **1991**, *15*, 153–180; b) D. Philp, J. F. Stoddart, *Angew. Chem.* **1996**, *108*, 1242–1286; *Angew. Chem. Int. Ed. Engl.* **1996**, *35*, 1154–1196.

  1433-7851/99/3811-1600 $ 17.50+.50/0

[3] a) H. Rau in *Photochromism, Molecules and Systems* (Eds.: H. Dürr, H. Bouas-Laurent), Elsevier, Amsterdam, **1990**, pp. 165 – 192; b) V. Balzani, F. Scandola, *Supramolecular Photochemistry*, Ellis Horwood, New York, **1991**, pp. 355 – 394.

[4] I. Cabrera, M. Engel, L. Häussling, C. Mertesdorf, H. Ringsdorf, in *Frontiers in Supramolecular Organic Chemistry and Photochemistry* (Eds.: H.-J. Schneider, H. Dürr), VCH, Weinheim, **1991**, pp. 311 – 336.

[5] For host – guest systems with photoswitchable hydrogen bonding see, for example, a) F. Würthner, J. Rebek, Jr., *Angew. Chem.* **1995**, *107*, 503 – 505; *Angew. Chem. Int. Ed. Engl.* **1995**, *34*, 446 – 448; b) J. Rosengaus, I. Willner, *J. Phys. Org Chem*. **1995**, *8*, 54 – 62.

[6] For host – guest systems with metal ions see, for example, a) S. Shinkai in *Comprehensive Supramolecular Chemistry* (Eds.: J. L. Atwood, J. E. D. Davis, D. D. MacNicol, F. Vögtle), Pergamon, Oxford, **1996**; b) H. Shinmori, M. Takeuchi, S. Shinkai, *J. Chem. Soc. Perkin Trans. 2*, **1998**, 947 – 852.

[7] Other examples: a) S. Anderson, T. D. W. Claridge, H. L. Anderson, *Angew. Chem*. **1997**, *109*, 1367 – 1370, *Angew. Chem. Int. Ed. Engl.* **1997**, *36*, 1310 – 1313; b) H. Murakami, A. Kawabuchi, K. Kotoo, M. Kunitake, N. Nakashima, *J. Am. Chem. Soc*. **1997**, *119*, 7605 – 7606.

[8] For enzyme catalysis see, for example, I. Willner, *Acc. Chem. Res.* **1997**, *30*, 347 – 356, and references therein.

[9] For dendrimeric materials see, for example, a) A. Archut, F. Vögtle, L. De Cola, G. C. Azzellini, V. Balzani, P. S. Ramanujam, R. H. Berg, *Chem. Eur. J.* **1998**, *4*, 688 – 706; b) D. M. Junge, D. V. McGrath, *Chem. Commun*. **1997**, 857 – 858; c) D.-L. Jiang, T. Aida, *Nature* **1997**, *388*, 454 – 456.

[10] For liquid crystalline materials see, for example, T. Ikeda, O. Tsutsumi, *Science* **1995**, *268*, 1873 – 1875.

[11] For polymeric materials see, for example, a) G. S. Kumar, D. C. Neckers, *Chem. Rev.* **1989**, *89*, 1915 – 1925; b) I. Willner, S. Rubin, *Angew. Chem*. **1996**, *108*, 401 – 418, *Angew. Chem. Int. Ed. Engl.* **1996**, *35*, 367 – 385.

[12] For peptide systems see, for example, a) L. Ulysse, J. Cubillos, J. Chmielewski, *J. Am. Chem. Soc*. **1995**, 117, 8466 – 8467; b) R. H. Berg, S. Hvilsted, P. S. Ramanujam, *Nature* **1996**, *338*, 505 – 508; c) R. Cerpa, F. E. Cohen, I. D. Kuntz, *Folding Des.* **1996**, *1*, 91 – 101; d) S. Rudolph-Böhner, M. Krüger, D. Oesterhelt, L. Moroder, T. Nägele, J. Wachtveitl, *J. Photochem. Photobiol. Chem. A*, **1997**, *105*, 235 – 248; e) O. Pieroni, A. Fissi, G. Popova, *Prog. Polym. Sci.* **1998**, *23*, 81 – 123.

[13] a) M. R. Ghadiri, K. Kobayashi, J. R. Granja, R. K. Chadha, D. E. McRee, *Angew. Chem*. **1995**, *34*, 76 – 78; *Angew. Chem. Int. Ed. Engl.* **1995**, *34*, 93 – 95; b) K. Kobayashi, J. R. Granja, M. R. Ghadiri, *Angew. Chem*. **1995**, *34*, 79 – 81; *Angew. Chem. Int. Ed. Engl.* **1995**, *34*, 95 – 98; c) T. D. Clark, M. R. Ghadiri, *J. Am. Chem. Soc*. **1995**, *117*, 12364 – 12365; d) T. D. Clark, J. M. Buriak, K. Kobayashi, M. P. Isler, D. R. McRee, M. R. Ghadiri, *J. Am. Chem. Soc.* **1998**, *120*, 8949 – 8962.

[14] The required linear octapeptide [H(D-^{Me}*N*-Ala-L-(*p*-MeBlz)Cys-(D-^{Me}*N*-Ala-L-Phe)$_3$-COOH] was prepared by solid-phase methods and cleaved from the resin by basic hydrolysis. After cyclization in solution and removal of the cysteine protecting group, the resulting cyclic peptide was alkylated with 4,4′-(bromomethyl)azobenzene to give **1** after RP-HPLC purification. MS (ESI): m/z: 1977 [M+H$^+$], (calcd: 1976.9).

[15] For analytical investigations the peptide solutions in CH_2Cl_2 were dried over molecular sieves. After removal of the CH_2Cl_2 **1** was dissolved in $CHCl_3$ and $CDCl_3$ (previously dried over P_2O_5).

[16] Solutions of (*E*)-**1** in chloroform in daylight contain small amounts of (*Z*)-**1** (*E*:*Z* = 90:10, as determined by ^{1}H NMR spectroscopy).

[17] Irradiation at 366 nm was performed with a 4 W UV lamp. At a concentration of 0.05 mM the photostationary equilibrium was obtained after 5 min.

[18] See, for example, U. Funke, H.-F. Grützmacher, *Tetrahedron* **1987**, *43*, 3787 – 3795.

[19] ^{1}H NMR spectroscopic data shows 4,4′-dimethylazobenzene, for example, has an *E*:*Z* ratio of 20:80 at the photostationary equilibrium (UV irradiation with 366 nm).

[20] Irradiation with visible light was performed with a 15 W fluorescence lamp (Philips F15T8/CW). At a concentration of 0.05 mM the photostationary equilibrium was obtained after 20 min.

[21] ^{1}H NMR data for (*Z*)-**1** (400 MHz, 293 K, ca. 3 mM in $CDCl_3$): L-Phe^1**:** 8.68 (d, J = 9.1 Hz, NH); 5.32 (m, CH); 2.88 – 3.04 (m, C$^\beta$H$_2$); 7.14 – 7.25 (m, C$^{\delta,\varepsilon,\xi}$H); D-^{Me}*N*-Ala^2: 2.79 (s, NCH$_3$); 5.85 (q, J = 6.5 Hz, C-H); 1.03 (d, J = 6.8 Hz, C$^\beta$H$_3$); L-Phe^3: 8.72 (d, J = 8.7 Hz, NH); 5.27 (m, C$^\alpha$H); 2.88 – 3.04 (m, C$^\beta$H$_2$); 7.14 – 7.25 (m, C$^{\delta,\varepsilon,\xi}$H); D-^{Me}*N*-Ala^4: 2.76 (s, NCH$_3$); 5.89 (overlap., C$^\alpha$H); 0.98 (d, J = 7.0 Hz, C$^\beta$H$_3$); L-Phe^5: 8.69 (d, J = 8.7 Hz, NH); 5.29 (m, C$^\alpha$H); 2.88 – 3.04 (m, C$^\beta$H$_2$); 7.14 – 7.25 (m, C$^{\delta,\varepsilon,\xi}$H); D-^{Me}*N*-Ala^6: 2.76 (s, NCH$_3$); 5.75 (q, J = 7.0 Hz, C$^\alpha$H); 0.92 (d, J = 7.0 Hz, C$^\beta$H$_3$); L-Cys^7: 8.41 (d, J = 8.6 Hz, NH); 5.19 (m, C$^\alpha$H); 2.67 (2.18, m, C$^\beta$H$_2$); 3.56 (br s, SC*H*$_2$C$_6$H$_4$N=); 7.07 (d, J = 8.1 Hz, SCH$_2$C$_6$H$_4$N=); 6.56 (d, J = 8.1 Hz, SCH$_2$C$_6$H$_4$N=); D-^{Me}*N*-Ala^8: 3.43 (s, NCH$_3$); 5.89 (overlap., C$^\alpha$H); 1.23 (d, J = 7.0 Hz, C$^\beta$H$_3$).

[22] J. M. Sanders, B. K. Hunter, *Modern NMR Spectroscopy*, 2nd ed., Oxford University Press, Oxford, **1993**.

[23] ^{1}H NMR data of (*E*)-**1** (500 MHz, 293 K, ca. 3 mM in $CDCl_3$): δ = 8.42 – 8.81 (m, NH of L-Phe and L-Cys in H bond); 7.70 – 7.85 (m, L-Cys SC*H*$_2$C$_6$H$_4$N=); 7.32 – 7.50 (m, L-Cys SCH$_2$C$_6$H$_4$N=); 7.14 – 7.24 (m, L-Phe C$^{\delta,\varepsilon,\xi}$H); 7.08 – 7.15 (m, free NH of L-Phe and L-Cys); 4.57 – 5.92 (m, L-Phe, L-Cys, and D-^{Me}*N*-Ala C$^\alpha$H); 2.52 – 3.80 (m, L-Phe, L-Cys C$^\beta$H$_2$, L-Cys SC*H*$_2$C$_6$H$_4$N=, D-Me*N*-Ala NCH$_3$); 0.84 – 1.28 (m, D-Me*N*-Ala C$^{\beta H3}$).

[24] C. Steinem, A. Janshoff, M. S. Vollmer, M. R. Ghadiri, *Langmuir*, in press.

A Chiral Molecular Based Metamagnet Prepared from Manganese Ions and a Chiral Triplet Organic Radical as a Bridging Ligand**

Hitoshi Kumagai and Katsuya Inoue*

The design of molecular materials with interesting optical and/or magnetic properties has been one of the major challenges of the last few years.[1, 2] In 1984 Barron and Vrbancich gave the name "magneto-chiral dichroism" (MChD) to the relationship between natural optical activity and magnetic field induced circular dichroism.[3] In 1997 Rikken and Raupach observed the MChD effect for tris-(3-trifluoroacetyl-(±)-camphorato)europium(III) in the paramagnetic state.[4] The MChD effect depends on the magnitude of the magnetic moment. It is important to make fully chiral molecule-based magnets, which are expected to exhibit a strong MChD effect. Although novel properties are expected for such compounds, there are only a few examples of molecule-based chiral magnetic material.[1, 5–7]

Recently, a strategy of using π-conjugated polynitroxide radicals with high-spin ground states as bridging ligands for magnetic metal ions was applied to assemble and align electron spins on a macroscopic scale.[8–11] The crystal structures and the magnetic structures of these complexes

[*] Prof. Dr. K. Inoue, Dr. H. Kumagai
Institute for Molecular Science
Nishigounaka 38, Myoudaiji
Okazaki 444 – 8585 (Japan)
Fax: (+81) 564-54-2254
E-mail: kino@ims.ac.jp

[**] We thank Professor Hideaki Kanno (Shizuoka University) for measurement of the optical rotation. This work was supported by a Grant-in-Aid for Scientific Research on Priority Areas (no. 10146102) from the Ministry of Education, Science Sports and Culture, Japan.